Effect of tantalum addition on the tensile properties of V-Ta-4Cr-4Ti quaternary alloys

Takeshi Miyazawa[1]*, Yoshimitsu Hishinuma[2], Takuya Nagasaka[2] and Takeo Muroga[2]

[1]Tohoku University, Sendai, 980-8579 Japan

[2]National Institute for Fusion Science, Toki, Gifu, 509-5292, Japan

Abstract

Various V-Ta-4Cr-4Ti quaternary alloys containing different amounts of Ta were investigated to determine the effect of Ta concentration on their tensile properties. Six button-shaped ingots of V-*x*Ta-4Cr-4Ti alloys (x = 4, 8, 15, 22, 24, and 35 wt.%) were fabricated on a laboratory scale by using non-consumable arc-melting in argon atmosphere. The sheet specimens for all the V-Ta-4Cr-4Ti alloys examined herein were obtained by cold-rolling; hot-rolling or intermediate annealing was not required. Although the examined alloys were fabricated on a laboratory scale, the high-Ta alloys, unlike the high-Cr alloys, did not experience crack formation in the cold rolling process. It is possible that V-4Cr-4Ti alloys adopt large amount of Ta and its strengthening effect without negative impact on rolling fabricability. Tensile strength tended to increase with increasing Ta content at both room temperature and high temperatures of 973 K and 1073 K, which can be attributed to the solid solution strengthening by Ta. Thus, addition of Ta to V-4Cr-4Ti alloys can improve their strength without decreasing their rolling fabricabilities. However, an alloy containing excess Ta (V-35Ta-4Cr-4Ti) showed a loss of ductility and a brittle fracture mode due to the formation of a large amount of friable Laves phase. Therefore, it is necessary to limit the amount of Ta to prevent the formation of the Laves phase.

Keywords

blanket structural materials, tensile properties, solid solution strengthening

1. Introduction

Vanadium-based alloys are attractive blanket structural materials for advanced fusion reactors because of their inherently low-induced radioactivity, their high strength at elevated temperatures, and their good resistance against neutron irradiation damage [1,2]. An alloy of V containing 4wt.% Cr and 4wt.% Ti (V-4Cr-4Ti) has been recognized as the leading candidate for this purpose [3,4]. High temperature strength is one of the key factors that determines the upper operating temperature, which is currently assumed to be approximately 973 K for this alloy [5]. Although the solid solution strengthening provided by higher Cr content can improve the high temperature strength of V-Cr-Ti alloys, it may result in reduced ductility and fabricability [6, 7]. The effects of solute elements on the mechanical properties of V-based binary alloys containing Al, Ti, Cr, Fe, Nb, Mo, and Ta have been previously reported [8]. Ta has relatively low long-lived radioactivity after exposure to fusion neutrons [9]. It also has favorable properties such as a large strengthening effect in solid solutions, and V-Ta binary alloys containing ≤ 20 wt.% of Ta exhibit good fabricability [8, 10, 11]. Although V-(5–20)Ta-(5–20)Ti ternary alloys and V-10Ta ternary alloys containing Al, Cr, and Mo have been investigated [11, 12], V-Ta-Cr-Ti quaternary alloys have not yet been studied. The purpose of this study was to clarify the effect of Ta addition on the tensile properties of V-4Cr-4Ti alloys for fusion reactor applications.

2. Experimental procedures

Table 1 lists the chemical compositions of the V-4Cr-4Ti ternary alloy and various V-Ta-4Cr-4Ti quaternary alloys examined in this study. V-4Cr-4Ti is a high purity reference alloy known as HIFS-HEAT-2, which was developed by the National Institute for Fusion Science (NIFS) and fabricated in the form of ingots by electron beam melting and vacuum arc re-melting on a 166 kg scale [13, 14]. The amount of interstitial impurities such as O, N, and C in the V-Ta-4Cr-4Ti quaternary alloys were controlled to give the same levels as those seen in the V-4Cr-4Ti ternary alloy. Six different V-*x*Ta-4Cr-4Ti (x = 4, 8, 15, 22, 24, 35 wt.%) alloys were fabricated by non-consumable arc-melting technique under an argon atmosphere to obtain button-shaped ingots, each weighing approximately 10 g. The button-shaped ingots were cold-rolled into sheets with a thickness of 0.25 mm, representing a >90% reduction in thickness. The V-35Ta-4Cr-4Ti alloy was expected to be friable, as the addition of >9 at.% Ta results in a Laves phase (V_2Ta) in the V-Ta phase diagram [15]. However, the alloy was found to be ductile, and was cold-rolled to a sheet.

X-ray diffraction (XRD) spectrometry was used to characterize the presence of secondary phases within the matrix and determine the lattice parameters of the alloys after annealing at 1273 K. The operating voltage and electron current were 40 kV and 50 mA, respectively. The sheet specimens for Vickers microhardness measurements were cut from the alloy sheets, mechanically and electrolytically polished, and then annealed at 1173–1473 K for 3.6 ks under a pressure of less than 1×10^{-4} Pa. Vickers microhardness (HV) measurements were performed at room temperature (RT), with an indentation load of 4.9 N (500 gf), and a dwell time of 30 s. The hardness was calculated by averaging the results obtained from ten indents. The tensile tests were conducted at NIFS to investigate the tensile properties of V-Ta-4Cr-4Ti quaternary alloys, including yield stress (YS), ultimate tensile strength (UTS), uniform elongation (UE), total elongation (TE), and reduction in area (RA). Flat-plate specimens, also

known as SS-J tensile specimens [16], were used for the tensile tests, and had a gauge length of 5 mm, gauge width of 1.2 mm, and thickness of 0.25 mm. The loading axis of the specimens was parallel to the L direction (rolling direction) of the plates. The tensile tests along the L direction were conducted under a pressure of less than 1×10^{-4} Pa at an initial strain rate of 6.67×10^{-4} s^{-1} at three different temperatures, RT, 973 K, and 1073 K. Microstructural observations were performed using transmission electron microscopy (TEM) and scanning electron microscopy (SEM). Disk specimens with diameter of 3 mm were electropolished with 20% sulfuric acid solution using a twin-jet polishing machine to make thin film for TEM.

Table 1. Chemical compositions of the examined alloys.

Code	Scale	V	Ta mass% (at.%)	Cr mass% (at.%)	Ti mass% (at.%)	C mass ppm	N mass ppm	O mass ppm
V-4Cr-4Ti	166 kg	bal.	0.0016 (0.0004)	4.02 (3.93)	4.15 (4.41)	120	90	120
V-4Ta-4Cr-4Ti	10 g	bal.	3.80 (1.10)	3.89 (3.91)	3.95 (4.31)	70	60	140
V-8Ta-4Cr-4Ti	10 g	bal.	8.37 (2.50)	3.91 (4.07)	3.96 (4.47)	60	70	150
V-15Ta-4Cr-4Ti	10 g	bal.	14.5 (4.55)	3.87 (4.22)	3.94 (4.67)	80	70	140
V-22Ta-4Cr-4Ti	10 g	bal.	21.6 (7.18)	3.88 (4.49)	3.97 (4.99)	70	60	140
V-24Ta-4Cr-4Ti	10 g	bal.	23.8 (8.07)	3.86 (4.55)	3.99 (5.11)	60	80	120
V-35Ta-4Cr-4Ti	10 g	bal.	35.4 (13.3)	3.82 (5.01)	3.99 (5.68)	70	60	130

3. Results

3.1. XRD analysis

Figure 1 shows the XRD spectra of the V-22Ta-4Cr-4Ti and V-35Ta-4Cr-4Ti alloys after annealing at 1273 K. Laves phases (V_2Ta) were identified in both the alloys, with the peaks for the Laves phase of V-35Ta-4Cr-4Ti being slightly sharper than those of V-22Ta-4Cr-4Ti. The V (200) peaks shift toward lower angles with increasing Ta content. The lattice parameters of the V matrix were calculated from these shifts using Bragg's equation and are plotted in Figure 2. It is considered likely that the lattice parameter increased with increase in Ta content because Ta was dissolved in the V matrix.

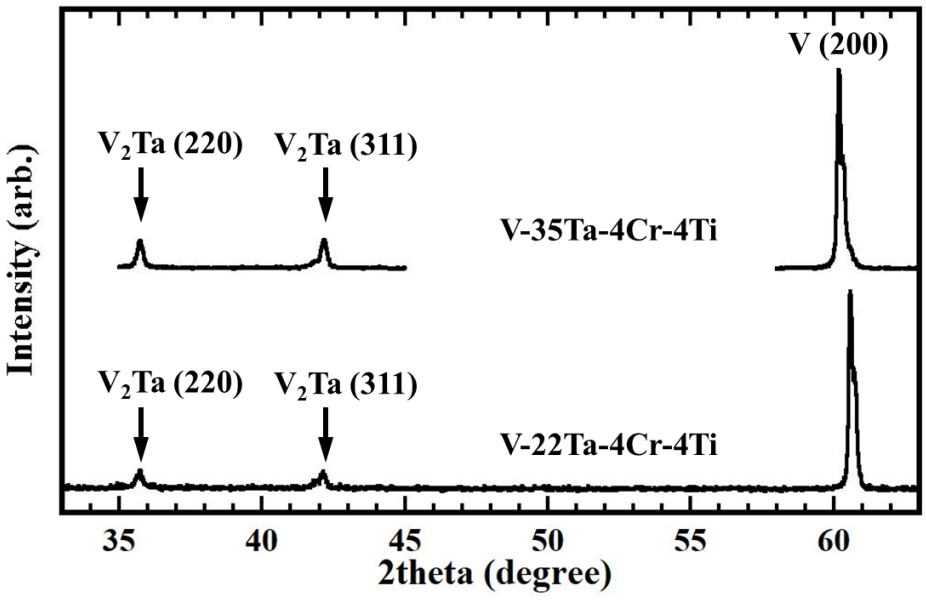

Figure 1. XRD spectra of the V-22Ta-4Cr-4Ti and V-35Ta-4Cr-4Ti alloys after annealing at 1273 K.

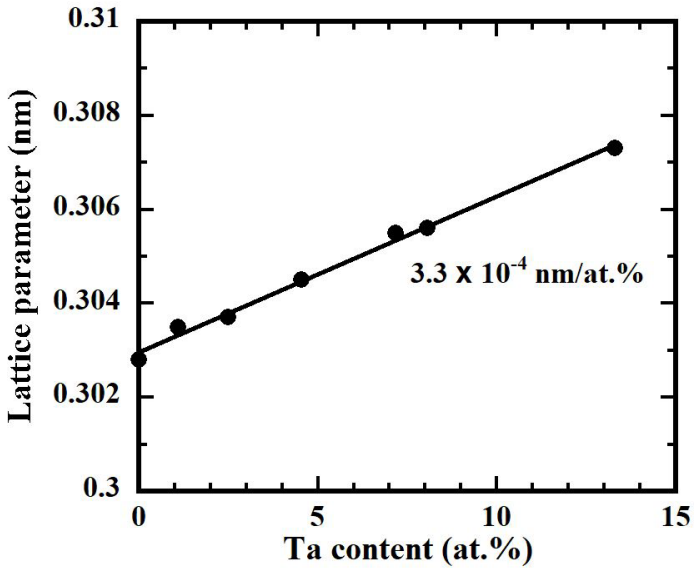

Figure 2. Change in the lattice parameter of the V matrix with increase in Ta content.

3.2. Hardness and recrystallization

Figure 3 shows the hardness recovery as a function of annealing temperature after cold rolling. It was found that the hardness increased with increase in Ta content. While V-4Ta-4Cr-4Ti, V-8Ta-4Cr-4Ti, and V-15Ta-4Cr-4Ti showed minimum hardness values after annealing at 1273 K, the minimum hardness of V-22Ta-4Cr-4Ti occurred after annealing at 1373 K. Figure 4 shows the SEM images of the grain structures of annealed V-Ta-4Cr-4Ti alloys. V-4Ta-4Cr-4Ti and V-8Ta-4Cr-4Ti were entirely recrystallized at 1273 K; however, V-22Ta-4Cr-4Ti was recrystallized at 1373 K. The recrystallized grains were elongated parallel to the cold-rolling direction. The mixed grain structures composed of both fine recrystallized grains and coarse recrystallized grains were observed. The recrystallization temperatures of the alloys were determined from their minimum-hardness temperature and microstructure observations. The recrystallization temperatures of V-4Ta-4Cr-4Ti, V-8Ta-4Cr-4Ti, and V-15Ta-4Cr-4Ti were determined to be 1273 K, while those of V-22Ta-4Cr-4Ti and V-24Ta-4Cr-4Ti were 1373 K. Thus, the recrystallization temperature increased with increasing Ta content. All the tensile specimens were annealed at their respective recrystallization temperatures. As the recrystallization temperature of V-35Ta-4Cr-4Ti was unclear, the tensile specimens of this alloy were annealed at 1373 K.

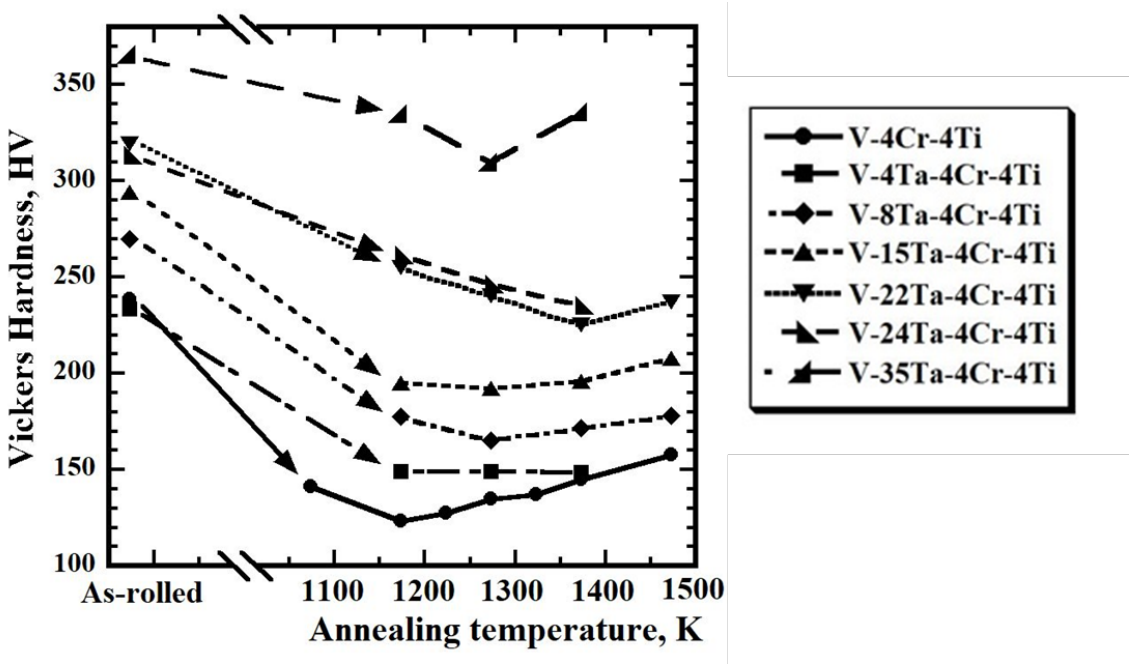

Figure 3. Recovery of hardness as a function of the annealing temperature after cold rolling.

The hardness data for V-4Cr-4Ti (NIFS-HEAT-2) has been plotted for reference [17].

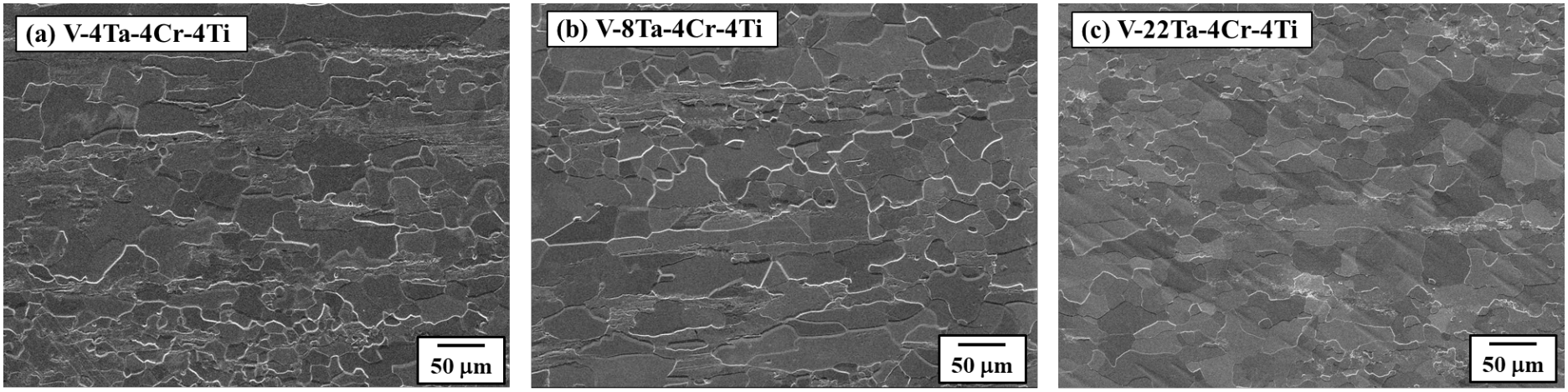

Figure 4. SEM images of the grain structures of (a) V-4Ta-4Cr-4Ti annealed at 1273 K, (b) V-8Ta-4Cr-4Ti annealed at 1273 K and (c) V-22Ta-4Cr-4Ti annealed at 1373 K.

3.3. Tensile properties

Figure 5 summarizes the engineering stress-strain curves of the V-4Cr-4Ti and V-Ta-4Cr-4Ti alloys obtained at RT, 973 K, and 1073 K. At 973 K, V-4Cr-4Ti and V-Ta-4Cr-4Ti alloys containing 15 wt.% or less of Ta exhibited serrated deformation curves. This deformation behavior indicates dynamic strain aging (DSA), which is manifested as oscillations in the flow stress on the tensile curves [18, 19]. Figure 6 shows that YS and UTS are linearly dependent on the Ta content. The hardening coefficients per unit of the Ta content were 41, 31, and 25 MPa/at.% at RT, 973 K, and 1073 K, respectively. Figure 7 shows the dependence of UE and TE on the Ta content and demonstrates that elongation gradually decreased with increasing Ta content, with the addition of 15 at.% Ta causing a sharp drop in elongation. Figures 8 and 9 show SEM images of the fracture surfaces of V-8Ta-4Cr-4Ti, V-22Ta-4Cr-4Ti, and V-35Ta-4Cr-4Ti obtained at RT. V-8Ta-4Cr-4Ti and V-22Ta-4Cr-4Ti had reductions in area (RA) of 92 % and 83 %, respectively, and dimples were observed on the fractographs, as shown in Figure 9 (a) and (b), which is typical of ductile fractures. The fracture surface of V-35Ta-4Cr-4Ti exhibited no necking and an RA of 0 %, indicating loss of ductility and a brittle fracture mode. Figure 10 shows the SEM images of the fracture surfaces of V-8Ta-4Cr-4Ti, V-22Ta-4Cr-4Ti, and V-35Ta-4Cr-4Ti obtained at 973 K. V-8Ta-4Cr-4Ti, V-22Ta-4Cr-4Ti, and V-35Ta-4Cr-4Ti had an RA of 89 %, 77 %, and 55 %, respectively.

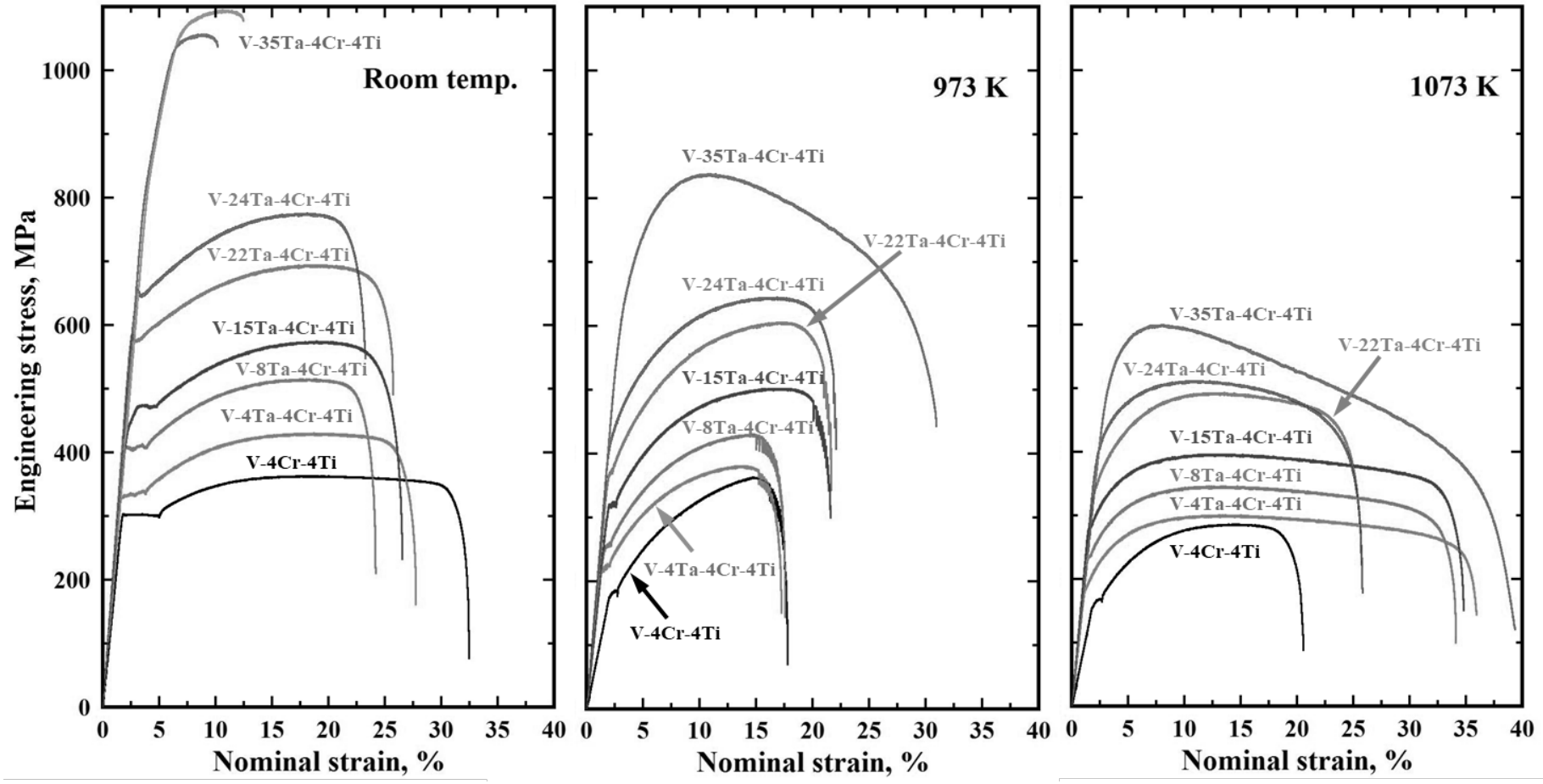

Figure 5. Stress-strain curves of the V-4Cr-4Ti and V-Ta-4Cr-4Ti alloys at RT, 973 K, and 1073 K. Tensile tests for V-35Ta-4Cr-4Ti at RT were conducted twice to confirm their reproducibility.

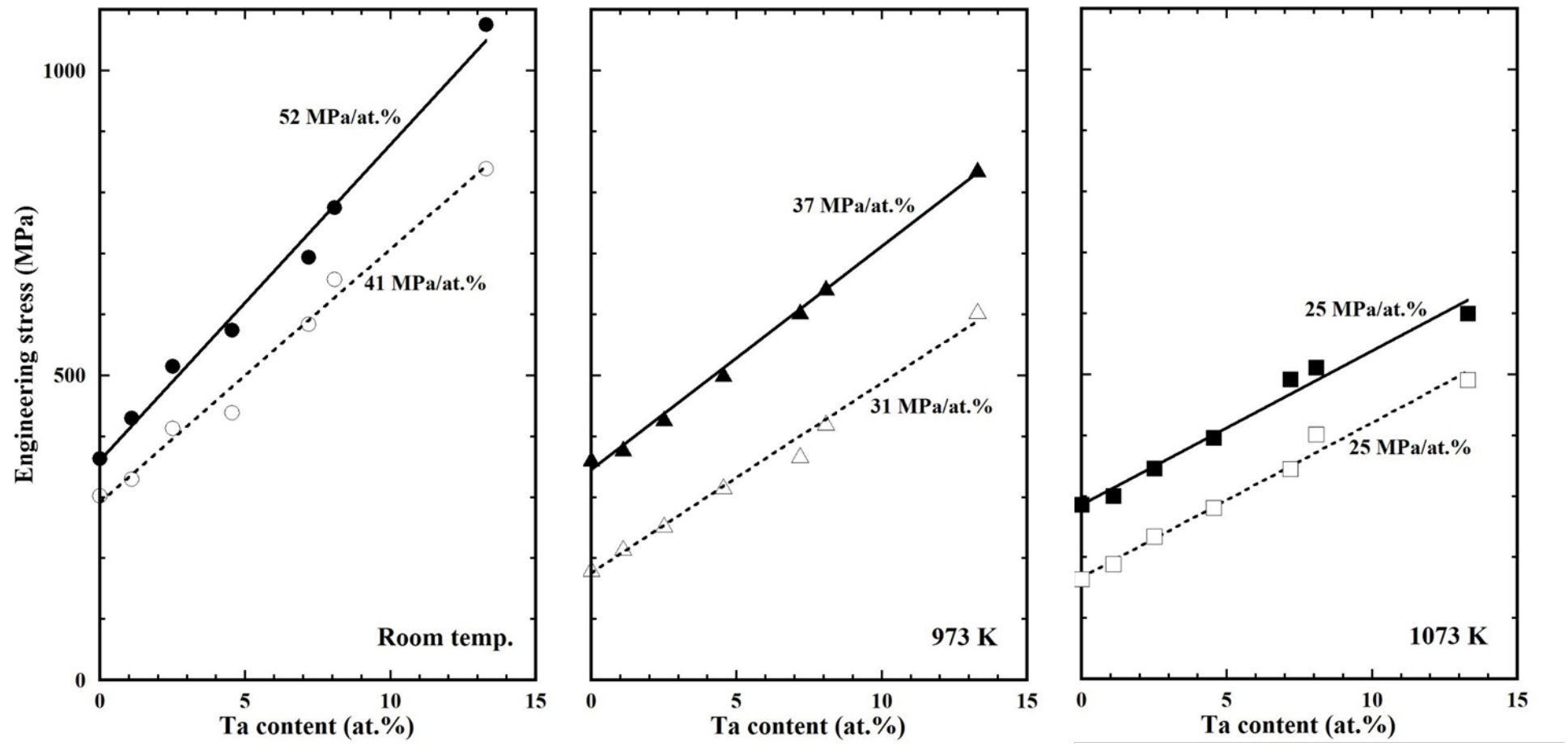

Figure 6. Dependence of yield stress (YS, open symbols) and ultimate tensile strength (UTS, closed symbols) on Ta content.

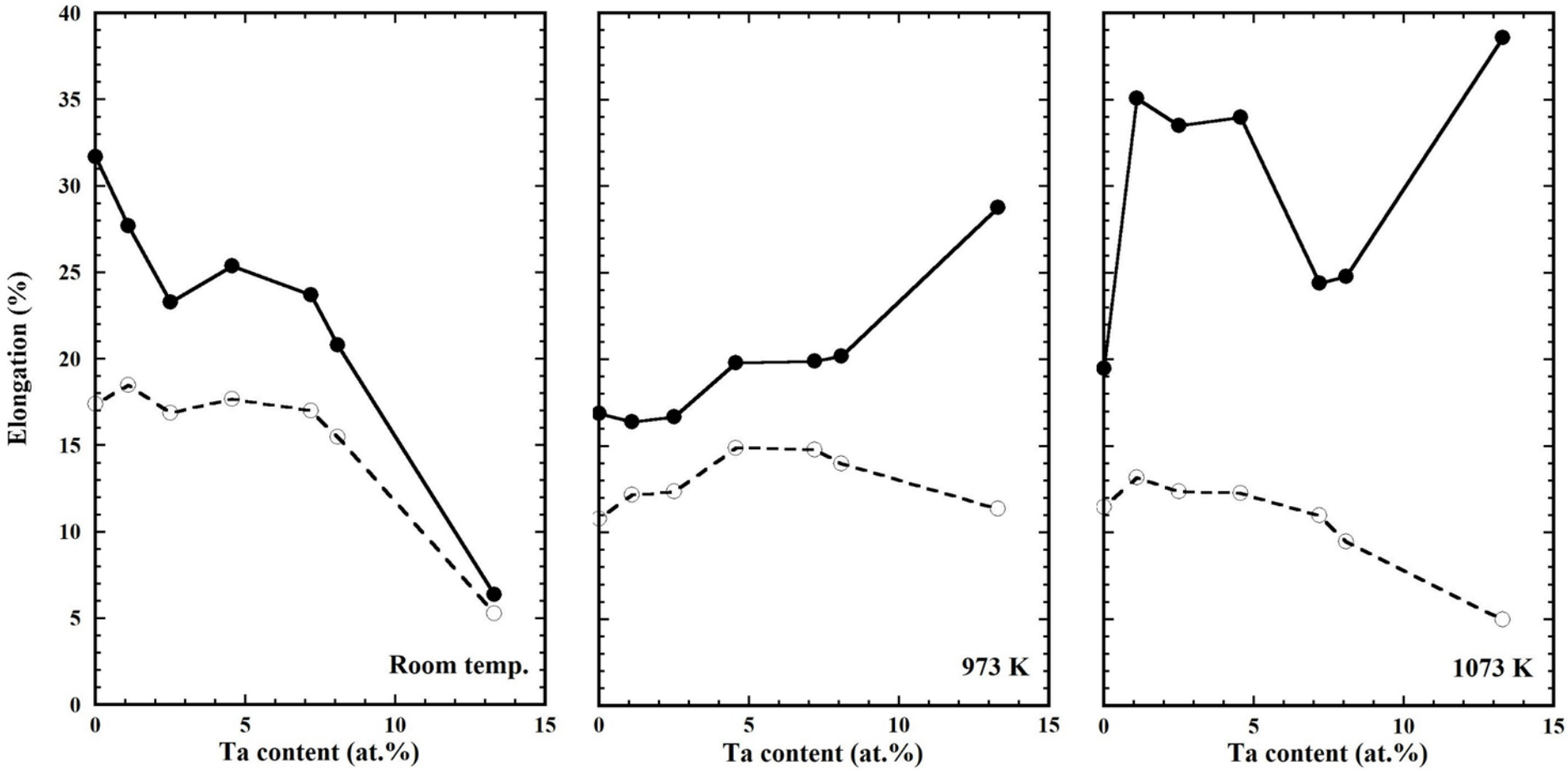

Figure 7. Dependence of uniform elongation (UE, open symbols) and total elongation (TE, closed symbols) on Ta content.

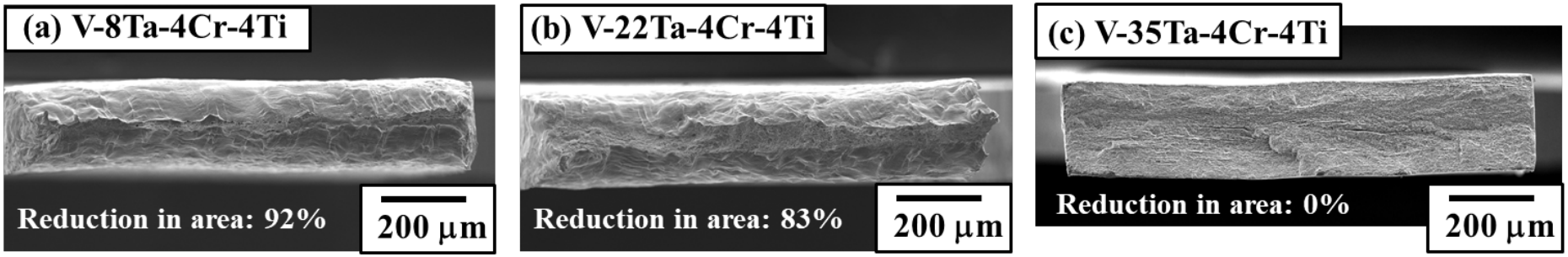

Figure 8. SEM images of the fracture surfaces of (a) V-8Ta-4Cr-4Ti, (b) V-22Ta-4Cr-4Ti and (c) V-35Ta-4Cr-4Ti at RT.

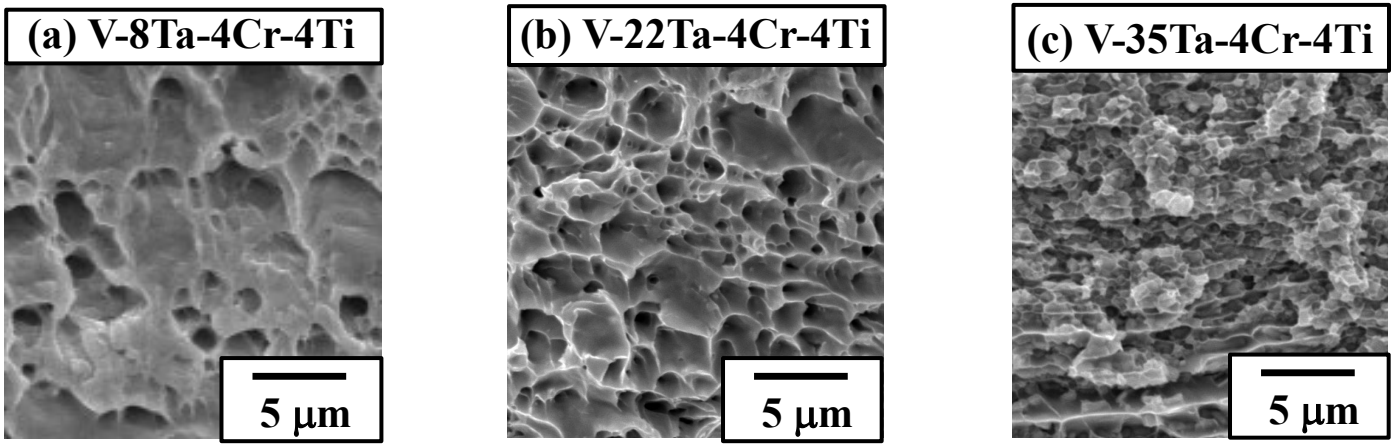

Figure 9. Magnified SEM images of the fracture surfaces of (a) V-8Ta-4Cr-4Ti, (b) V-22Ta-4Cr-4Ti and (c) V-35Ta-4Cr-4Ti at RT.

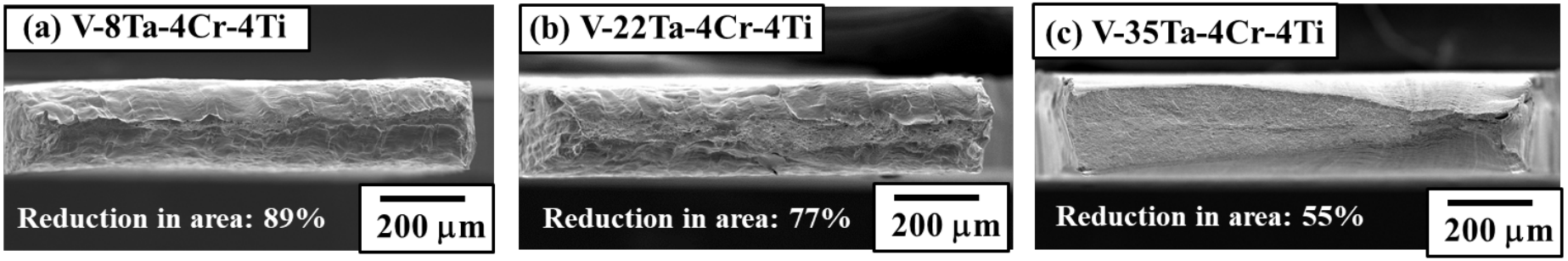

Figure 10. SEM images of the fracture surfaces of (a) V-8Ta-4Cr-4Ti, (b) V-22Ta-4Cr-4Ti and (c) V-35Ta-4Cr-4Ti at 973K.

3.4. Microstructural observations

Figure 11 presents the bright field TEM images of V-22Ta-4Cr-4Ti and V-35Ta-4Cr-4Ti annealed at 1373 K. V-22Ta-4Cr-4Ti was found to contain precipitates with sizes of 0.1–0.5 μm, which were considered Ti-rich precipitates [17, 20]. More precipitates were observed in V-35Ta-4Cr-4Ti than in V-22Ta-4Cr-4Ti. It is considered that the precipitates of the Laves phase (V_2Ta) were formed in addition to the Ti-rich precipitates in V-35Ta-4Cr-4Ti.

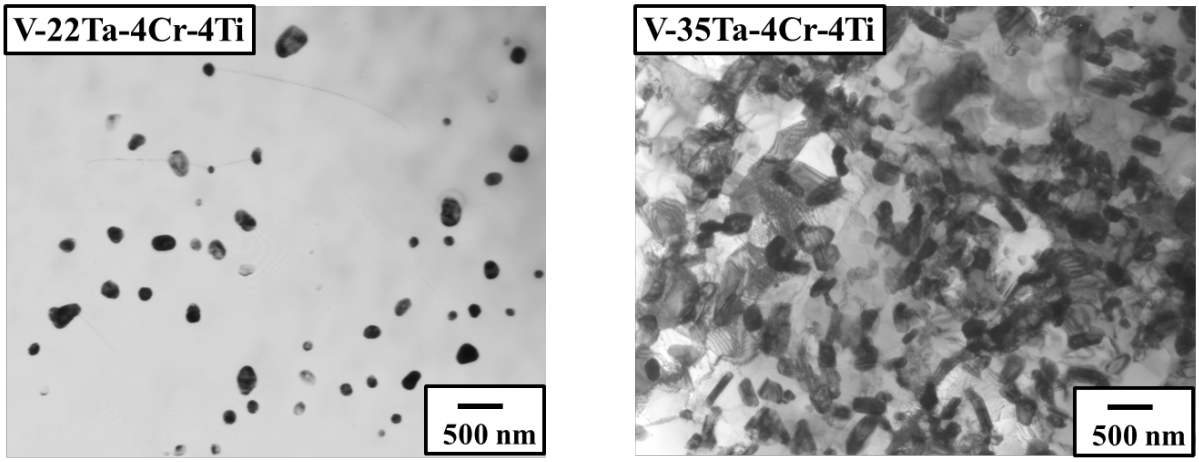

Figure 11. TEM images of the V-22Ta-4Cr-4Ti and V-35Ta-4Cr-4Ti alloys annealed at 1373 K.

4. Discussion

In the V-Ta-4Cr-4Ti quaternary alloys, the YS and UTS tended to increase with increasing Ta content at all temperatures studied. As the Ta content increased, the strength increased due to strengthening of the solid solution by Ta. True fracture stress was calculated from RA and nominal fracture stress as summarized in Table 2. The true fracture stress values of V-8Ta-4Cr-4Ti and V-22Ta-4Cr-4Ti obtained at RT were over 2000 MPa. This estimation means that the V alloy matrix at RT was work-hardened up to 2000 MPa and finally fractured with ductile dimples. Up to a Ta content of 22 wt.%, even if the Laves phase was formed, the number density of the precipitates was small, such that there was almost no effect on the tensile properties. However, the true fracture stress of V-35Ta-4Cr-4Ti was much lower than that of V-8Ta-4Cr-4Ti and V-22Ta-4Cr-4Ti. It is considered that V-35Ta-4Cr-4Ti alloy contained excess Ta, as shown in Figure 11, resulting in a reduction in the fracture stress due to the formation of a large amount of the friable Laves phase. Therefore, it is necessary to limit the amount of Ta to prevent the formation of the Laves phase. All the V-Ta-4Cr-4Ti alloys examined in this study had favorable rolling fabricabilities, as sheet specimens with thickness of 0.25 mm were obtained by cold-rolling, illustrating that hot-rolling or intermediate annealing were not required. Although the addition of a large amount of Cr to V and its alloys leads to reduced rolling fabricabilities [7, 8, 21], addition of Ta to V-4Cr-4Ti alloys was shown to increase the strength without negatively impacting the rolling fabricability. At RT, V-22Ta-4Cr-4Ti and V-24Ta-4Cr-4Ti alloys showed higher YS than that of the high-Cr alloy V-20Cr-4Ti (~500 MPa) [22]. However, previous studies on high-Cr V-Cr-Ti alloys reported that ductile-to-brittle transition temperature (DBTT) tended to increase due to both solid solution strengthening by Cr and formation of large Ti-rich precipitates. This study revealed that the addition of Ta improves the tensile strength at RT, 973 K and 1073 K in the V-Ta-4Cr-4Ti quaternary alloys along with an increase in DBTT, which is one of the key factors that

determines the lower operating temperature limit [5], due to the solid solution strengthening by Ta. It is necessary to further investigate whether the addition of Ta itself has an advantage to expand the operation design window by conducting Charpy impact tests and creep tests.

Phase stabilities of 8–12Cr ferritic steels such as 12Cr-1Mo-V-W (HT9), 9Cr-1Mo-V-Nb (T-91), and 8Cr-2W-V-Ta (F82H) have previously been investigated, and showed Laves phase (Fe_2Mo, Fe_2W) formation during long-term aging [23]. The large Laves phase precipitates formed at grain boundaries during long-term aging caused the degradation of Charpy impact properties, such as embrittlement [24, 25]. While the Laves phase (V_2Ta) was identified in V-22Ta-4Cr-4Ti (Fig. 1), it did not significantly affect the tensile properties of V-22Ta-4Cr-4Ti. However, long-term aging may result in coarsening of the Laves phase, causing decrease in ductility. Thus, long-term aging and creep tests of the V-Ta-4Cr-4Ti quaternary alloys will be required in the future to characterize the material stability and determine the optimum Ta content.

Table 2. Estimation of the true fracture stress.

Code	Room temperature	973 K
V-8Ta-4Cr-4Ti	2760 MPa	1280 MPa
V-22Ta-4Cr-4Ti	2960 MPa	1470 MPa
V-35Ta-4Cr-4Ti	1060 MPa	980 MPa

5. Summary

The effect of Ta addition on the tensile properties of V-*x*Ta-4Cr-4Ti alloys (x = 4, 8, 15, 22, 24, and 35 wt.%) was investigated. All the V-Ta-4Cr-4Ti alloys examined in this study allowed sheet specimens to be obtained by cold-rolling without requiring hot-rolling or intermediate annealing. Although the examined alloys were fabricated on a laboratory scale, the high-Ta alloys did not experience cracks in the cold rolling process as seen in the high-Cr alloys. It is possible that thicker plates may possess larger fabricability. Tensile strength tended to increase with Ta content at both RT and higher temperatures of 973 K and 1073 K. As the Ta content increased, strength also increased due to the solid solution strengthening by Ta. Addition of Ta to V-4Cr-4Ti alloys can therefore improve strength without degrading rolling fabricabilities. An alloy containing excess Ta (V-35Ta-4Cr-4Ti) showed reduced ductility and a brittle fracture mode due to the formation of a large amount of the friable Laves phase. Therefore, it is necessary to limit the amount of Ta to prevent formation of the Laves phase.

Acknowledgment

This work is performed under the auspices of the NIFS Collaboration Research Program (NIFS20KEMF172) and JSPS KAKENHI, Grant Number 18K13523.

References

[1] D.L. Smith, B.A. Loomis and D.R. Diercks: J. Nucl. Mater. **135** (1985) 125-139.

[2] D.L. Smith, H.M. Chung, B.A. Loomis, H. Matsui, S.N. Votinov and W. Van Witzenburg: Fusion Eng. Des. **29** (1995) 399-410.

[3] H. Matsui, K. Fukumoto, D.L. Smith, H.M. Chung, W. Van Witzenburg and S.N. Votinov: J. Nucl. Mater. **233-237** (1996) 92-99.

[4] D.L. Smith, H.M. Chung, B.A. Loomis and H.-C. Tsai: J. Nucl. Mater. **233-237** (1996) 356-363.

[5] S.J. Zinkle and N.M Ghoniem: Fusion Eng. Des. **51-52** (2000) 55-71.

[6] B.A Loomis, H.M. Chung, L.J. Nowicki and D.L. Smith: J. Nucl. Mater. **212-215** (1994) 799-803.

[7] K. Sakai, M. Satou, M. Fujiwara, K. Takahashi, A. Hasegawa and K. Abe: J. Nucl. Mater. **329-333** (2004) 457-461.

[8] N. Iwao, T. Kainuma, T. Suzuki and R. Watanabe: J. Less-Common Met. **83** (1982) 205-217.

[9] S. Cierjacks, K. Ehrlich, E.T. Cheng, H. Conrads and H. Ullmaier: Nucl. Sci. Eng. **106** (1990) 99-113.

[10] N. Iwao, T. Kainuma, R. Watanabe and T. Shimomura: Trans. Jan. Inst. Met. **20** (1979) 172-180.

[11] B.R. Rajala and R.J. VanThyne: J. Less-Common Met. **3** (1961) 489-500.

[12] N. Iwao, T. Kainuma, T. Suzuki and R. Watanabe: J. Less-Common Met. **83** (1982) 219-225.

[13] T. Nagasaka, T. Muroga, M. Imamura, S. Tomiyama and M. Sakata: Fusion Technol. **39** (2001) 659-663.

[14] T. Nagasaka, T. Muroga, Y. Wu and M. Imamura: J. Plasma Fusion Res. SERIES **5** (2002) 545-550.

[15] Phase diagrams of binary vanadium alloys, edited by J.F. Smith, ASM International.

[16] A. Kohyama, K. Hamada and H. Matsui: J. Nucl. Mater. **179-181** (1991) 417-420.

[17] N.J. Heo, T. Nagasaka and T. Muroga: J. Nucl. Mater. **325** (2004) 53-60.

[18] D.T. Hoelzer and A.F. Rowcliffe: J. Nucl. Mater. **307-311** (2002) 596-600.

[19] T. Miyazawa, T. Nagasaka, Y. Hishinuma, T. Muroga, Y. Li, Y. Satoh, S. Kim and H. Abe: J. Nucl. Mater. **442** (2013) S341-S345.

[20] T. Nagasaka, N.J. Heo, T. Muroga and M. Imamura: Fusion Eng. Des. **61-62** (2002) 757-762.

[21] T. Miyazawa, T. Muroga and Y. Hishinuma: J. Plasma Fusion Res. SERIES **11** (2015) 89-93.

[22] M. Fujiwara, T. Sakamoto, M. Satou, A. Hasegawa, K. Abe, K. Kaiuchi and T. Furuya: Mater. Trans. 46 (3) (2005) 517-521.

[23] M. Tamura, H. Hayakawa, A. Yoshitake, A. Hishinuma and T. Kondo: J. Nucl. Mater. **155-157** (1988) 620-625.

[24] M. Tamura, K. Shinozuka, H. Esaka, S. Sugimoto, K. Ishizawa and K. Masamura: J. Nucl. Mater. **283-287** (2000) 667-671.

[25] K. Shiba, H. Tanigawa, T. Hirose, H. Sakasegawa and S. Jitsukawa: Fusion Eng. Des. **86** (2011) 2895-2899.